



PERGAMON

Transportation Research Part B 36 (2002) 405–419

---

---

TRANSPORTATION  
RESEARCH  
PART B

---

---

www.elsevier.com/locate/trb

# A new continuum model for traffic flow and numerical tests

Rui Jiang, Qing-Song Wu <sup>\*</sup>, Zuo-Jin Zhu

*Institute of Engineering Science, University of Science and Technology of China, Hefei 230026,  
People's Republic of China*

Received 31 March 2000; received in revised form 24 December 2000; accepted 3 January 2001

---

## Abstract

A new continuum traffic flow model is developed in this paper based on an improved car-following model. In this new continuum model, the speed gradient replaces the density gradient in the equation of motion, and this replacement guarantees the property that the characteristic speeds are always less than or equal to the macroscopic flow speed. This new model also overcomes the backward travel problem that exists in many high-order continuum models. Shock waves, rarefaction waves, stop-and-go waves, and local cluster effects can be obtained from this new model and are consistent with the diverse nonlinear dynamical phenomena observed in the freeway traffic. © 2002 Elsevier Science Ltd. All rights reserved.

*Keywords:* Traffic flow; Continuum model; Characteristic speed; Car-following

---

## 1. Introduction

Continuum traffic flow models are needed for understanding the collective behavior of traffic, designing efficient control strategies, developing macroscopic traffic simulation, and, etc. The study of continuum traffic flow models began with the LWR model developed independently by Lighthill and Whitham (1955) and Richards (1956). The LWR model is known as the simple continuum model, in which the relationships among three aggregate variables – traffic density, flow rate, and space mean speed are modeled. The LWR model employs the conservation equation in the following form:

$$\frac{\partial k}{\partial t} + \frac{\partial q}{\partial x} = g(x, t) \quad (1)$$

and is supplemented by the fundamental equation of traffic flow

---

<sup>\*</sup> Corresponding author. Tel.: +86-551-3601-272; fax: +86-551-3631-760.  
*E-mail address:* qswu@ustc.edu.cn (Q.-S. Wu).

$$q = uk \quad (2)$$

and a relationship between the mean speed and the traffic density under equilibrium conditions

$$u = u_e(k). \quad (3)$$

In the above equations  $q$  is the flow rate of the traffic stream,  $k$  is the traffic density,  $u$  is the space mean speed, and  $g(x, t)$  is the generation rate, while  $t$  and  $x$  represent time and space, respectively.

Using the simple continuum model, a variety of simple traffic flow problems can be reproduced analytically by the method of characteristics (Lighthill and Whitham, 1955) and numerically by finite differences (Michalopoulos et al., 1984). However, as pointed out by Liu et al. (1998), since the speed in this model is determined by the equilibrium speed–density relationship (Eq. (3)), no fluctuation of speed around the equilibrium values is allowed, the model does not faithfully describe nonequilibrium traffic flow dynamics. Moreover, the simple continuum model does not have the ability to explain the amplification of small disturbances on heavy traffic because no stability condition can be derived from the model. Therefore, from the theoretical point of view, the simple continuum model does not adequately describe traffic flow dynamics.

In order to overcome the shortcomings in the simple continuum model, Payne (1971) introduced a high-order continuum traffic flow model that includes a dynamics equation in addition to the continuity equation. The dynamics equation is derived from car-following theory and has the following form:

$$\frac{\partial u}{\partial t} + u \frac{\partial u}{\partial x} = -\frac{v}{kT} \frac{\partial k}{\partial x} + \frac{u_e - u}{T}, \quad (4)$$

where  $T$  is the relaxation time, and  $v = -0.5\partial u_e/\partial k$  is the anticipation coefficient. The left-hand side of Eq. (4) represents the acceleration. The first term on the right-hand side is called the anticipation term, which is used to reflect the fact that drivers react to traffic conditions in front of them. The second term on the right-hand side represents a relaxation to equilibrium, that is, the deviation from the equilibrium speed–density relationship.

Payne's model represents an improvement over the simple continuum model as it incorporates the momentum equation and takes the acceleration and inertia effects into account. As a result, the model can describe the amplification of small disturbances in heavy traffic and allow fluctuations of speed around the equilibrium values. Thus, it does overcome some deficiencies in the simple continuum model. However, as pointed out by Daganzo (1995), in Payne's model there always exists a characteristic speed that is greater than the macroscopic flow velocity. This means that the future conditions of a traffic flow will be affected by the traffic conditions behind the flow. One fundamental principle of traffic flow is that vehicles are anisotropic and respond only to frontal stimuli. That is, a vehicle is influenced only by the motion of vehicles in front of it, not by the motion of vehicles behind it. However, this fundamental principle is violated in Payne's model.

A few other high-order continuum models have been developed hereafter among which are Papageorgiou's high-order model (Papageorgiou et al., 1989), Michalopoulos' viscous model (Michalopoulos et al., 1991) and semi-viscous model (Michalopoulos et al., 1993), and others (Phillips, 1978; Kühne, 1984; Ross, 1988). Recently, Zhang (1998) presented a non-equilibrium model and addressed the issue of specifying high-order continuum models that have appropriate characteristic disturbance propagation speeds. Although these models represent some improvements over Payne's model in some aspects, they do not resolve the characteristic speed issue that

exists in Payne's model and hence the problem that one characteristic speed is greater than the macroscopic flow velocity remains intact in all of them.

In this paper, we develop a new macroscopic continuum model by introducing an improved car-following theory and applying the usual connection method of macro–micro variables. The new continuum model overcomes the problem of a characteristic speed being greater than the macroscopic flow velocity and therefore can describe the traffic flow dynamics more realistically.

The remainder of the paper is organized as follows. In Section 2, we present an improved car-following model built upon the existing car-following models. In Section 3, we develop a new continuum model based on the improved car-following model. In Section 4, we analyze the wrong-way travel problem existing in Payne's model and show how the new model overcomes this problem. In Section 5, we analyze some qualitative properties of the model, including linear stability and the existence of smooth traveling waves. In Section 6, we present the numerical scheme of the model. We then analyze the shock waves and the rarefaction waves in Section 7 and the local cluster effects in Section 8. We conclude the paper in Section 9.

## 2. An improved car-following model

The car-following model was developed to model the motion of vehicles following each other on a single lane without overtaking. It is assumed that a driver responds, through accelerations or decelerations, to the car in front of it. In the course of car-following, the dynamic state of the following car is determined by the speeds of the leading car and the following car itself, the distance between the two cars, the road conditions, the capability of the car, the personality of the driver and so on. Due to the complexity of the problem, drivers and cars are often assumed to be homogeneous and road conditions ideal. The classical car-following theory (Gazis et al., 1961) is represented by the following equation:

$$\frac{dv_{n+1}(t + \Delta t)}{dt} = \lambda \Delta v, \quad (5)$$

where  $\Delta v = v_n(t) - v_{n+1}(t)$ , with  $v_n$  and  $v_{n+1}$  being the speeds of the leading car and the following car, respectively; and  $\Delta t$  is the reaction time.  $\lambda$  is the sensitivity and is given by

$$\lambda = a \frac{[v_{n+1}(t + \Delta t)]^m}{(\Delta x)^l}. \quad (5a)$$

In Eq. (5a),  $\Delta x = x_n(t) - x_{n+1}(t)$ , where  $x_n$  and  $x_{n+1}$  are the positions of the leading car and the following car, respectively;  $a$  is a positive coefficient of proportionality; and  $m$  and  $l$  are non-negative parameters. In this model, the distance between successive vehicles can be arbitrarily close when the leading and the following cars have identical speed. Apparently this is unrealistic. Therefore, the classical car-following model cannot describe the dynamic state of a single car correctly.

Bando et al. (1995) argued that there are two types of theories on regulations of car-following. The first type is based on the assumption that the driver of each vehicle seeks a safe following distance from its leading vehicle, which depends on the relative velocity of the two successive vehicles. The second type of theories assumes that the driver seeks a safe velocity determined by

the distance from the leading vehicle. Based on the latter assumption, Bando et al. (1995) proposed a car-following model called the optimal velocity model (OVM) as follows:

$$\frac{dv_{n+1}(t)}{dt} = \kappa[V(\Delta x) - v_{n+1}(t)], \quad (6)$$

where  $\kappa$  is a reaction coefficient,  $V(\Delta x)$  represents the legal velocity of the following car. We should notice that in Bando's model the time lag of response is not introduced.

Helbing and Tilch (1998) carried out a calibration of the OVM with respect to the empirical follow-the-leader data. They found that an extremely short relaxation time,  $T = 1/\kappa$ , could result in a very high value of acceleration, which led to an overshooting of the vehicle velocity. To improve the OVM, they developed a generalized force model (GFM). They believed that when  $\Delta v < 0$ , it is necessary to consider the acceleration caused by the relative speed of the successive cars. The GFM model has the following form:

$$\frac{dv_{n+1}(t)}{dt} = \kappa[V(\Delta x) - v_{n+1}(t)] + \lambda \Delta v H(-\Delta v), \quad (7)$$

where  $H$  is the Heaviside function ( $H(x) = 0$  where  $x \leq 0$  and  $H(x) = 1$  where  $x > 0$ ), and  $\lambda = \lambda(\Delta x, v_{n+1})$  is the sensitivity as in Eq. (5).

According to Treiber et al. (1999), there exists in the real world a common driver behavior that none of the existing car-following models can explain. That is, when the distance between two vehicles is shorter than the safe distance, the driver of the following vehicle may not decelerate if the preceding vehicle travels faster than the following vehicle because the headway between the two vehicles will become larger. We carry out a lot of observations to the real traffic and find out that the phenomenon does exist. Neither the OVM in Eq. (6) nor the GFM in Eq. (7) can explain this phenomenon. Given the observed car-following phenomena, we believe that the relative speed between the leading and the following vehicles,  $\Delta v$ , whether  $\Delta v < 0$  or  $\Delta v > 0$ , has an impact on the behavior of the following driver and therefore should be considered explicitly. Based on this assumption, we propose an improved car-following model as follows:

$$\frac{dv_{n+1}(t)}{dt} = \kappa[V(\Delta x) - v_{n+1}(t)] + \lambda \Delta v. \quad (8)$$

This model considers the effects of both the distance and the relative speed of two successive vehicles, theoretically it is more realistic and exact than those previous ones. Notice that this improved model combines both the classical car-following model in Eq. (5) and the OVM in Eq. (6). Therefore, both the classical car-following model and the OVM are the special cases of this new model. As in the OVM, the reaction time is also neglected in this new model. In future work, we plan to consider this factor.

### 3. A new continuum model

The improved car-following model we develop in the previous section describes the traffic flow conditions from a microscopic point of view. In order to develop the corresponding macroscopic continuum model, we need to transform the discrete variables of individual vehicles into the continuous flow variables. We assume that the state of the car  $n + 1$  at position  $x$  represents the

average traffic condition at  $[x - \frac{1}{2}\Delta, x + \frac{1}{2}\Delta]$ , which is determined by the average traffic condition in the preceding region  $[x + \frac{1}{2}\Delta, x + \frac{3}{2}\Delta]$ . Here  $\Delta$  corresponds to  $\Delta x$  in car-following theory, and it varies with different inter-vehicle spaces between different successive vehicles. Then we can transfer the microscopic variables to the macroscopic ones as follows (Liu et al., 1998):

$$v_{n+1}(t) \rightarrow u(x, t), \quad v_n(t) \rightarrow u(x + \Delta, t), \quad V(\Delta x) \rightarrow u_e(k(x, t)) \tag{9a}$$

and

$$\kappa \rightarrow 1/T, \quad \lambda \rightarrow 1/\tau, \tag{9b}$$

where  $T$  is the relaxation time and  $\tau$  is the time needed for the backward propagated disturbance to travel a distance of  $\Delta$ . Applying Eqs. (9a) and (9b) to the car-following model in Eq. (8), we have

$$\frac{du(x, t)}{dt} = \frac{u_e(k) - u(x, t)}{T} + \frac{u(x + \Delta, t) - u(x, t)}{\tau}. \tag{10}$$

Expanding the right-hand side of Eq. (10), and neglecting the high-order terms, we obtain

$$\frac{du}{dt} = \frac{u_e - u}{T} + \frac{\Delta}{\tau} \frac{\partial u}{\partial x}. \tag{11}$$

Define

$$c_0 = \Delta/\tau, \tag{12}$$

where  $c_0$  represents the propagation speed of the disturbance.

We also know that

$$\frac{du}{dt} = \frac{\partial u}{\partial t} + u \frac{\partial u}{\partial x}. \tag{13}$$

By substituting Eqs. (12) and (13) into Eq. (11), we have

$$\frac{\partial u}{\partial t} + u \frac{\partial u}{\partial x} = \frac{u_e - u}{T} + c_0 \frac{\partial u}{\partial x} \tag{14}$$

which is the equation of motion. Thus, the new improved continuum model we present above, consistent with other high-order models, comprises two partial differential equations as follows:

$$\frac{\partial k}{\partial t} + \frac{\partial(ku)}{\partial x} = g(x, t), \tag{15a}$$

$$\frac{\partial u}{\partial t} + u \frac{\partial u}{\partial x} = \frac{u_e - u}{T} + c_0 \frac{\partial u}{\partial x}. \tag{15b}$$

Comparing our new model with other high-order models in the previous literature, we can see that the new model differs from the others in the motion equation (Eq. (15b)), in which the speed gradient term replaces the density gradient term as the anticipation term. This replacement in the new model solves the characteristic speed problem that exists in the previous high-order models and therefore enables the new model to satisfy the anisotropic property of traffic flow. To see this, we next analyze the new model by the method of characteristics. We rewrite system (15a) and (15b) as follows:

$$\frac{\partial U}{\partial t} + [A] \frac{\partial U}{\partial x} = E, \tag{16}$$

where

$$U = \begin{bmatrix} k \\ u \end{bmatrix}, \quad [A] = \begin{bmatrix} u & k \\ 0 & u - c_0 \end{bmatrix}, \quad E = \begin{bmatrix} g \\ (u_e - u)/T \end{bmatrix}. \quad (17)$$

The eigenvalues,  $\lambda$ , of the  $[A]$  matrix are found by setting

$$\det |[A] - \lambda[I]| = 0, \quad (18)$$

where  $[I]$  is identity matrix. From Eq. (18), we have

$$\begin{vmatrix} u - \lambda & k \\ 0 & u - c_0 - \lambda \end{vmatrix} = 0 \quad (19)$$

thus  $\lambda_1 = u$ ,  $\lambda_2 = u - c_0$ . These are the characteristic speeds for our new model, i.e.

$$\left(\frac{dx}{dt}\right)_1 = u \quad \text{and} \quad \left(\frac{dx}{dt}\right)_2 = u - c_0. \quad (20)$$

Since  $c_0 \geq 0$ , it follows that the characteristic speeds  $dx/dt$  are always less than or equal to the macroscopic flow velocity  $u$ . In other words, the new continuum model does not have any characteristic speed greater than the macroscopic flow velocity. This property is significant because the fundamental principle that vehicles are anisotropic and respond only to frontal stimuli is incorporated in the new model.

More importantly, as we will see in the next section, the new model overcomes the wrong-way travel problem (Daganzo, 1995) existing in the previous high-order models. In addition, the new model satisfies the stability feature of traffic flow, which will be shown in Section 8.

#### 4. Wrong-way travel analysis

In this section we will study whether or not there is any negative travel speed (wrong-way travel) problem in our new model. Daganzo (1995) considered the time evolution of the rear of a stopped queue without any arriving traffic. The situation is formally described by the following initial/boundary conditions:

$$u = 0 \quad \text{and} \quad k = k_m H(x) \quad \text{for} \quad x \leq A \quad \text{and} \quad t = 0 \quad (A > 0), \quad (21a)$$

$$u = 0 \quad \text{for} \quad x = A \quad \text{and} \quad t > 0, \quad (21b)$$

where  $H$  is the Heaviside function, and  $k_m$  is the jam density.

Under the above initial conditions the correct solution should be that nothing would happen, as predicted by the LWR model. However, we cannot obtain this result from Payne's model. This can be verified easily by setting  $u$  and its derivatives to zero in Eq. (4):

$$u_e - \frac{v}{k} \frac{\partial k}{\partial x} = 0 \quad (22)$$

Rewrite Eq. (22) as

$$v \frac{\partial k}{\partial x} = u_e k = q_e. \quad (23)$$

In addition, the number of vehicles within the region of  $(-\infty, A)$  must remain constant

$$\int_{-\infty}^A k \, dx = k_m A. \tag{24}$$

From Eqs. (23) and (24), as  $t \rightarrow \infty$ , there is a S-shaped equilibrium profile centering around  $x = 0$ , which means that vehicles move backward (see Fig. 1, Daganzo, 1995).

In contrast, such backward-travel problem does not exist in the new model. To verify this, we solve the new model under the initial condition of (21a) and (21b). Setting  $u$  and its derivatives to zero in Eq. (15b), we have

$$u = u_e \tag{25}$$

which is obviously true in region  $(-\infty, A)$ . This result is consistent with the prediction of the LWR model.

The previous analyses can help us find the reason why the wrong-way travel problem exists in Payne’s model but not in the LWR model or the new model. In the LWR model, no fluctuation around the equilibrium value is allowed. The equilibrium speed–density relationship is a monotonically decreasing function. This means that the density gradient is negative if the speed gradient is positive and vice versa. The acceleration equation of the LWR model can be derived as follows (Pipes, 1969):

$$\frac{du}{dt} = -k \left( \frac{\partial u_e}{\partial k} \right)^2 \frac{\partial k}{\partial x}. \tag{26}$$

The kinetic wave speed of the simple model

$$c_k = \frac{dq_e}{dk} = u + k \frac{du_e}{dk}.$$

Since

$$\frac{du_e}{dk} \leq 0$$

is always hold, if the speed at position  $x$  equals zero, then

$$c_k = k \frac{du_e}{dk} \leq 0,$$

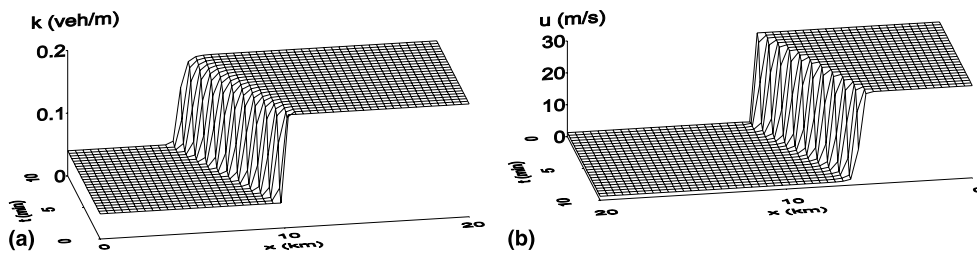


Fig. 1. Shock waves under the Riemann initial condition of (43a): (a) temporal development of density  $k(x, t)$ ; (b) temporal development of speed  $u(x, t)$ . In (b), the direction of the space and the time axes are reversed for illustrative purpose.

i.e. the state at position  $x$  is determined by what is downstream. Hence, we adopt the downstream one-sided speed gradient, which must be non-negative because the minimum speed is zero at any point and time. Since the density gradient has an opposite sign of the speed gradient, the density gradient must then be non-positive. From Eq. (26), the acceleration is non-negative when the speed at position  $x$  is zero. Therefore, the speed at position  $x$  will not decrease when the speed is zero. This means that the negative speed will not occur.

In Payne's model, fluctuation around the equilibrium value is allowed and we cannot draw the conclusion that the density gradient and the speed gradient have opposite signs. Therefore, we need not to know the speed gradient, because whether the speed gradient is negative or positive, we could not determine the sign of density gradient. If the speed at  $x$  is zero, the acceleration at  $x$  under Payne's model can be derived from Eq. (4) as follows:

$$\frac{du}{dt} = \frac{u_e}{T} - \frac{v}{kT} \frac{\partial k}{\partial x}. \quad (27)$$

If

$$\frac{\partial k}{\partial x} > \frac{u_e k}{v} \quad (28)$$

is satisfied, the acceleration will be negative. In this situation, the speed at position  $x$  will decrease from zero and therefore a negative speed will occur. This proves that Payne's model may trigger a negative speed even though the initial speed is non-negative.

In the new model, the speed gradient replaces the density gradient. From Eq. (15b), we have

$$\frac{du}{dt} = \frac{u_e}{T} + c_0 \frac{\partial u}{\partial x} \quad (29)$$

when the speed at position  $x$  becomes zero. From Eq. (20), here the two characteristic speeds are both non-positive, therefore, the state at the position  $x$  is determined only by what is downstream as in the simple model. The downstream one-sided speed gradient is adopted, which is non-negative, i.e.  $\partial u / \partial x \geq 0$ . Therefore, the acceleration must be non-negative. As a result, the speed will never decrease from zero and a negative speed could never exist in this new model. The replacement of the speed gradient as the anticipation term thus eliminates the mechanism that triggers a negative speed in Payne's model.

## 5. Qualitative properties of the model

Before the numerical computations are carried out, it is always preferred to tell some qualitative features of the model first. Therefore, in this section, we analyze linear stability and wave structure of the solution of the new model.

### 5.1. Linear stability analysis

Assuming  $g(x, t) = 0$ , and  $k_0$  and  $u_0 = u_e(k_0)$  are the steady-state solutions of Eqs. (15a) and (15b),  $k = k_0 + \xi$  and  $u = u_0 + \eta$  are perturbed solutions of Eqs. (15a) and (15b), with  $\xi = \xi(x, t)$  and  $\eta = \eta(x, t)$  small perturbations to the steady-state solutions. Next we discuss how these

perturbations evolve over time. Substituting the perturbed solutions  $k = k_0 + \xi$ ,  $u = u_0 + \eta$  into (15a) and (15b), then taking Taylor series expansions of the perturbed equations at  $k_0$  and  $u_0$ , and neglecting higher order terms of  $\xi$  and  $\eta$ , we obtain the following linearized equations:

$$\xi_t + u_0 \xi_x + k_0 \eta_x = 0, \tag{30a}$$

$$\eta_t + u_0 \eta_x = \frac{u'_e(k_0) \xi - \eta}{T} + c_0 \eta_x, \tag{30b}$$

where  $u'_e = du_e/dk$ . One can eliminate  $\eta$  from Eqs. (30a) and (30b) and obtain

$$(\partial_t + c \partial_x) \xi = -T[(\partial_t + c_1 \partial_x)(\partial_t + c_2 \partial_x) \xi], \tag{31}$$

where  $c = (ku)'|_{k=k_0} = u_0 + k_0 u'_e(k_0)$  is the kinematic wave speed, and  $c_1 = u_0 - c_0$ ,  $c_2 = u_0$ . According to the traditional way of linear stability analysis, substituting  $\xi(x, t) = \xi_0 \exp i(\gamma x - \omega t)$  into (31), we can show that

$$(-i\omega + ic\gamma) \xi = -T[(-i\omega + c_1 i\gamma)(-i\omega + c_2 i\gamma)] \xi. \tag{32}$$

For  $\xi$  to be non-trivial solution of (32), we must have

$$(-i\omega + ic\gamma) = -T[(-i\omega + c_1 i\gamma)(-i\omega + c_2 i\gamma)]. \tag{33}$$

It is obvious that the solution is stable if and only if the imaginary part of both of the roots  $\omega$  is non-positive. It is easily verified that the requirement for this is

$$c_1 \leq c \leq c_2. \tag{34}$$

When condition (34) is violated, traffic instability will occur, which leads to many kinds of complex traffic phenomena such as stop-and-go traffic. These are further discussed in Section 8.

### 5.2. Traveling wave and shock

In this subsection we study whether the new model smoothes out the shock waves of the LWR model. Considering a steady profile solution with a constant translational speed  $U$ :

$$k = k(X), \quad u = u(X), \quad X = x - Ut.$$

Substituting the steady profile solution into (15a) and (15b), still assuming  $g(x, t) = 0$ , we have

$$-Uk_X + (uk)_X = 0, \tag{35a}$$

$$T(u - c_0 - U)u_X = u_e - u. \tag{35b}$$

Integrating (35a) and reformulating, we have

$$u = U - \frac{A}{k}, \tag{36}$$

where  $A$  is a constant. Substituting (36) into (35b), and multiplying  $k$  on both sides, we obtain

$$-T(U - u)[U - (u - c_0)]k_X = q_e - Uk + A, \tag{37}$$

where  $q_e = u_e k$ . We are interested in solution curves between  $k_1$  at  $X = -\infty$  and  $k_2$  at  $X = +\infty$ . These values will be zeros of the right-hand side of (37), therefore  $k_X = 0$ . So,  $U$  and  $A$  must satisfy

$$q_e(k_1) - Uk_1 + A = q_e(k_2) - Uk_2 + A = 0, \tag{38}$$

thus

$$U = \frac{q_e(k_1) - q_e(k_2)}{k_1 - k_2}. \tag{39}$$

For a concave flow-density function  $q_e(k)$ , there may only exist steady compression waves, which implies  $k_1 < k_2$ . Moreover, a concave  $q_e(k)$  also guarantees that the right-hand side of (37) is always positive (Whitham, 1974; Del Castillo et al., 1994; Zhang, 1999). Therefore, when  $-T(U - u)[U - (u - c_0)]$  remains positive within  $(k_1, k_2)$ , then  $k_x > 0$  and we have a smooth traveling wave solution. Obviously solution to the inequality  $-T(U - u)[U - (u - c_0)] > 0$  is

$$u - c_0 < U < u. \tag{40}$$

When condition (40) is not satisfied,  $-T(U - u)[U - (u - c_0)]$  changes sign in the profile and a single-valued continuous profile is no longer possible, the profile turns back itself.

When this is the case, the analytical solution does not exist and it should be replaced by a weak solution consists of a discontinuity (i.e., a shock).

### 6. Numerical scheme

Assuming  $g(x, t) = 0$  and applying the finite difference method to discretize Eqs. (15a) and (15b), we obtain the following difference equations:

$$k_i^{j+1} = k_i^j + \frac{\Delta t}{\Delta x} k_i^j (u_i^j - u_{i+1}^j) + \frac{\Delta t}{\Delta x} u_i^j (k_{i-1}^j - k_i^j), \tag{41a}$$

(a) if the traffic is heavy ( $u_i^j < c_0$ ):

$$u_i^{j+1} = u_i^j + \frac{\Delta t}{\Delta x} (c_0 - u_i^j)(u_{i+1}^j - u_i^j) - \frac{\Delta t}{T} (u_i^j - u_e), \tag{41b}$$

(b) if the traffic is light ( $u_i^j \geq c_0$ ):

$$u_i^{j+1} = u_i^j + \frac{\Delta t}{\Delta x} (c_0 - u_i^j)(u_i^j - u_{i-1}^j) - \frac{\Delta t}{T} (u_i^j - u_e), \tag{41c}$$

where index  $i$  represents the road section and index  $j$  represents time. For the discretization of the conservation Eq. (41a), the difference format suitable for physical sense of traffic flow is applied (Papageorgiou, 1983). For the motion equations of (41b) and (41c), one-order upwind scheme is applied.

The numerical scheme in Eqs. (41a)–(41c) can maintain the physical properties of traffic flow even under extreme conditions. For example, assuming that at  $t = 0$ , the density of section  $i$  is zero,  $k_i^0 = 0$ , then we have

$$\frac{\partial k_i^0}{\partial t} = \frac{1}{\Delta x} [k_{i-1}^0 u_i^0 - k_i^0 u_{i+1}^0]. \tag{42a}$$

Since  $k_i^0 = 0$ ,  $k_i^0 u_{i+1}^0 = 0$ . Since  $k_{i-1}^0 u_i^0 \geq 0$  is always true, we have  $\partial k_i^0 / \partial t \geq 0$ . This implies that when  $t > 0$ ,  $k_i$  must be non-negative.

On the other hand, assuming that at  $t = 0$ , the density of section  $i$  is at maximum,  $k_i^0 = k_m$ , then we have

$$\lim_{k \rightarrow k_m} u_i^0 = \lim_{k \rightarrow k_m} u_e(k_i^0) = 0.$$

Therefore,  $k_{i-1}^0 u_i^0 = 0$  and  $k_i^0 u_{i+1}^0 \geq 0$ . Hence, from Eq. (42a),  $\partial k_i^0 / \partial t \leq 0$ , which guarantees that when  $t > 0$ ,  $k_i$  cannot be greater than the maximum jam density.

We can apply the same analyses to speed. Assuming that at  $t = 0$ , the speed of section  $i$  is zero,  $u_i^0 = 0$ , from Eq. (41b) we have

$$\frac{\partial u_i^0}{\partial t} = \frac{1}{\Delta x} c_0 u_{i+1}^0 + \frac{1}{T} u_e \geq 0 \tag{42b}$$

which guarantees that when  $t > 0$ ,  $u_i$  must be non-negative. Similarly, assuming that at  $t = 0$ , the speed of section  $i$  is at maximum,  $u_i^0 = u_f$ , from Eq. (41c) we have

$$\frac{\partial u_i^0}{\partial t} = \frac{1}{\Delta x} (c_0 - u_f)(u_f - u_{i-1}^0) - \frac{1}{T} (u_f - u_e) \leq 0 \tag{42c}$$

which implies that when  $t > 0$ ,  $u_i$  cannot be greater than the maximal value.

### 7. Shock waves and rarefaction waves

To evaluate whether the new model can represent important traffic flow conditions such as shock waves and rarefaction waves, we will carry out the numerical tests next. As pointed out by Daganzo (1995), the realistic description of shock fronts in traffic is a particularly difficult problem. We will investigate how the traffic flow fronts between a congested and a nearly free traffic evolve under two Riemann initial conditions. These two initial conditions are

$$k_u^1 = 0.04 \text{ (veh/m)}, \quad k_d^1 = 0.18 \text{ (veh/m)}, \tag{43a}$$

$$k_u^2 = 0.18 \text{ (veh/m)}, \quad k_d^2 = 0.04 \text{ (veh/m)}, \tag{43b}$$

where  $k_u$  and  $k_d$  are upstream and downstream densities, respectively. Condition (43a) corresponds to a situation where a nearly free-flow traffic meets a queue of nearly stopping vehicles, i.e., a shock wave situation. Condition (43b) corresponds to a situation of a dissolving queue, that is a rarefaction wave situation. Initial speed conditions are

$$u_u^{1,2} = u_e(k_u^{1,2}), \quad u_d^{1,2} = u_e(k_d^{1,2}). \tag{44a, b}$$

Free boundary conditions are used here, i.e.,  $\partial k / \partial x$  and  $\partial u / \partial x$  are equal to zero on both sides. The equilibrium speed–density relationship developed by Del Castillo and Benitez (1995) is applied

$$u_e = u_f \left[ 1 - \exp \left( 1 - \exp \left( \frac{c_m}{u_f} \left( \frac{k_m}{k} - 1 \right) \right) \right) \right], \tag{45}$$

where  $u_f$  is the free-flow speed;  $k_m$  is the maximum density; and  $c_m$  is the kinematic wave speed under the jam density. The test road section is 20 km long, and it is divided into 100 meshes equally, the time interval is 1 s. Parameter values used are as follows:

$$u_f = 30 \text{ m/s}, \quad k_m = 0.2 \text{ veh/m}, \quad T = 10 \text{ s}, \quad c_m = c_0 = 11 \text{ m/s}.$$

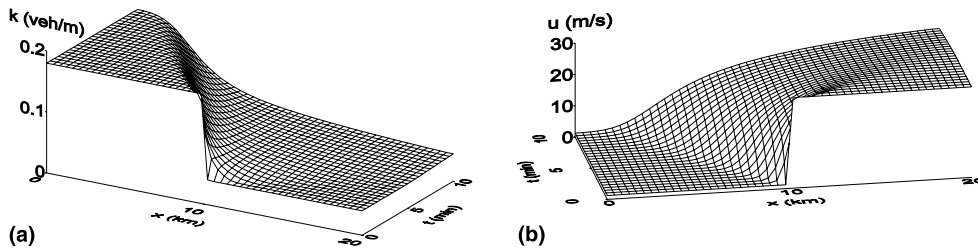


Fig. 2. Rarefaction waves under the Riemann initial condition of (43b): (a) temporal development of density  $k(x, t)$ ; (b) temporal development of speed  $u(x, t)$ .

The results under the two Riemann initial conditions of (43a) and (43b) are shown in Figs. 1 and 2, respectively.

From Figs. 1 and 2, we can see that the new model provides correct predictions under the two Riemann initial conditions of (43a) and (43b). Different Riemann initial conditions lead to different fronts between the congested and the free-flow traffic.

Substituting the value into (39) and (40), we can find out that inequality (40) is not satisfied under the initial condition (43a), which means that there should be a shock under the condition. And the propagation speed of the shock wave can be predicted negative from Eq. (39). Consistent with the analysis, Fig. 1 shows how the backward-moving shock wave front evolves.

Fig. 2 shows how the rarefaction wave front evolves. We can see that the moving front is smoothed over time and eventually leads to a continuous traffic flow, which is consistent with the reality.

## 8. Local cluster effect

The new model can also describe the amplification of a small disturbance, known as the local cluster effect of traffic flow (Kerner and Konhäuser, 1993, 1994; Herrmann and Kerner, 1998). The local cluster effect corresponds to the stop-and-go phenomena observed in the field due to a small disturbance. In this section, we simulate the local cluster effect with respect to a localized perturbation in an initial homogeneous condition. The following initial variation of the average density  $k_0$  is used as in (Herrmann and Kerner, 1998):

$$k(x, 0) = k_0 + \Delta k_0 \left\{ \cosh^{-2} \left[ \frac{160}{L} \left( x - \frac{5L}{16} \right) \right] - \frac{1}{4} \cosh^{-2} \left[ \frac{40}{L} \left( x - \frac{11L}{32} \right) \right] \right\}, \quad (46)$$

where  $L$  is the length of the road section under consideration. We let  $L = 32.2$  km and adopt the periodic boundary conditions as follows:

$$k(L, t) = k(0, t), \quad u(L, t) = u(0, t). \quad (47)$$

We next apply the equilibrium speed–density relationship proposed in (Kerner and Konhäuser, 1993):

$$u_e = u_f \left( 1 / \left( 1 + \exp \left\{ \frac{k/k_m - 0.25}{0.06} \right\} \right) - 3.72 \times 10^{-6} \right). \quad (48)$$

Assume the initial flow to be in local equilibrium everywhere, i.e.,  $u(x, 0) = u_e(k(x, 0))$ . Let  $\Delta k_0 = 0.01$  veh/m and the space interval be 100 m, the time interval is 1 s. Other parameter values are the same as in Section 7.

Substituting the values into the stable condition (34), we find out the traffic will be unstable when  $0.031 < k_0 < 0.084$ . Next we explore what the unstable traffic will evolve into, and the results are shown in Fig. 3(a)–(e).

In Fig. 3(a), the traffic flow density is very low, and hence the perturbation is dissipated without any amplification as we expect. As the initial density increases, small perturbations can be amplified, leading to traffic instability. Fig. 3(b) shows that when the density is just above the

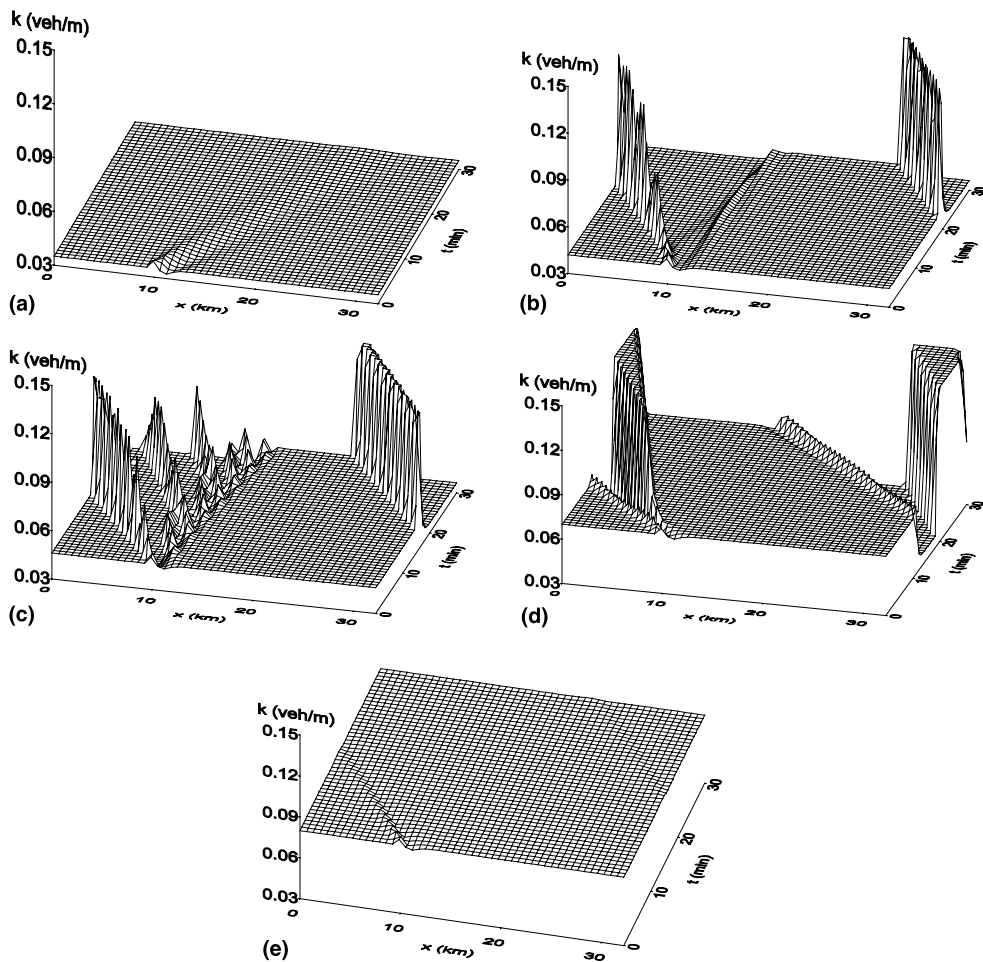


Fig. 3. Temporal evolution of traffic on a ring of 32.2 km circumference with a homogeneous initial traffic and a localized perturbation of amplitude  $\Delta k_0 = 0.01$  veh/m for: (a)  $k_0 = 0.035$  veh/m; (b)  $k_0 = 0.042$  veh/m; (c)  $k_0 = 0.046$  veh/m; (d)  $k_0 = 0.07$  veh/m; (e)  $k_0 = 0.08$  veh/m.

down-critical density,<sup>1</sup> a single local cluster forms. In Fig. 3(c), a complex localized structure consisting of two or more clusters forms as the density becomes higher. The situation of multiple clusters in Fig. 3(c) corresponds to a stop-and-go traffic. If the density increases even further, we observe a dipole-like structure as illustrated by Fig. 3(d). Finally, when the density becomes greater than the up-critical density, a stable regime is reached again as can be seen in Fig. 3(e). The above results are consistent with the properties of traffic flow found by Kerner and Konhäuser (1994), Herrmann and Kerner (1998) and Treiber et al. (1999). These local cluster effects are also consistent with the diverse nonlinear dynamics phenomena observed in realistic traffic flow.

## 9. Conclusions

Many existing continuum high-order models have a serious deficiency: in these models there exists a characteristic speed that is greater than the macroscopic flow velocity. In this paper, we present a new continuum model that does not have the characteristic speed problem as common in other continuum models. We first propose an improved car-following model that models the car-following behavior more realistically. We then develop a new continuum high-order model from the improved car-following model. In the new continuum model, the speed gradient replaces the density gradient as the anticipation term, and this replacement enables this new model to overcome the characteristic speed problem. The wrong-way travel issue does not exist in the new model. Linear stability analysis indicates that the model is sometimes unstable, and which leads to the formation of the complex traffic. It is also pointed out that similar with Payne model, the model also smoothes out the shock waves under certain condition. Finally, the numerical tests verify that the model is able to simulate complex traffic phenomena observed in the field such as shock waves, rarefaction waves, stop-and-go waves and local cluster effects. The results are consistent with the spectrum of nonlinear dynamic properties reported in the literature.

In our numerical tests, we assume that the disturbance propagation speed and the relaxation time are constants. In the future work we will carry out the calibration of the model parameters and examine the validation of the model using actual traffic data collected from the field.

## Acknowledgements

The authors are grateful to an anonymous referee for his suggestions to improve the paper. This work is supported by The National Natural Science Foundation of China (grant no. 19872062).

---

<sup>1</sup> There exist a down-critical and a up-critical density in the simulation. If the initial density is below down-critical density or above up-critical density, the traffic flow is stable, otherwise, the traffic flow is unstable. Theoretically the two densities should be 0.031 and 0.084, respectively. However, for the numerical error introduced by the numerical scheme, the two values are 0.04 and 0.077 in the simulation.

## References

- Bando, M., Hasebe, K., Nakayama, A., et al., 1995. Dynamical model of traffic congestion and numerical simulation. *Phys. Rev. E* 51, 1035–1042.
- Daganzo, C.F., 1995. Requiem for second-order fluid approximation of traffic flow. *Transp. Res.* 29B, 277–286.
- Del Castillo, J.M., Benitez, F.G., 1995. On functional form of the speed–density relationship – I: general theory, II: empirical investigation. *Transp. Res. B* 29, 373–406.
- Del Castillo, J.M., Pintado, P., Benitez, F.G., 1994. The reactive time of drivers and the stability of traffic flow. *Transp. Res. B* 28, 35–60.
- Gazis, D.C., Herman, R., Rothery, R.W., 1961. Nonlinear follow-the-leader models of traffic flow. *Oper. Res.* 9, 545–567.
- Helbing, D., Tilch, B., 1998. Generalized force model of traffic dynamics. *Phys. Rev. E* 58, 133–138.
- Herrmann, M., Kerner, B.S., 1998. Local cluster effect in different traffic flow models. *Physica A* 255, 163–188.
- Kerner, B.S., Konhäuser, P., 1993. Cluster effect in initially homogeneous traffic flow. *Phys. Rev. E* 48, R2335–2338.
- Kerner, B.S., Konhäuser, P., 1994. Structure and parameters of clusters in traffic flow. *Phys. Rev. E* 50, 54–83.
- Kühne, R.D., 1984. Macroscopic freeway model for dense traffic stop-start waves and incident detection. In: *Proceedings of the Ninth International Symposium on Transportation and Traffic Theory*, pp. 20–42.
- Lighthill, M.J., Whitham, G.B., 1955. On kinematic waves: II. A theory of traffic flow on long crowded roads. *Proc. R. Soc. London, Ser. A* 229 (1178), 317–345.
- Liu, G.Q., Lyrintzis, A.S., Michalopoulos, P.G., 1998. Improved high-order model for freeway traffic flow. *Transp. Res. Record* 1644, 37–46.
- Michalopoulos, P.G., Beskos, D.E., Lin, J.K., 1984. Analysis of interrupted traffic flow by finite difference methods. *Transp. Res. B* 18, 409–421.
- Michalopoulos, P.G., Yi, P., Beskos, D.E., et al., 1991. Continuum modeling of traffic dynamics. In: *Proceedings of the Second International Conference on Applications of advanced Technology in Transportation Engineering*, Minneapolis, pp. 36–40.
- Michalopoulos, P.G., Yi, P., Lyrintzis, A.S., 1993. Development of an improved high order continuum traffic flow model. *Transp. Res. Record* 1365, 125–132.
- Papageorgiou, M., 1983. Applications of automatic control concepts to traffic flow modeling and control. In: *Balakrishnan, A.V., Thoma, M. (Eds.), Lecture Notes in Control and Information Sciences*. Springer, Berlin, pp. 4–41.
- Papageorgiou, M., Blosseville, J.M., Hadj-Salem, H., 1989. Macroscopic modeling of traffic flow on the Boulevard Peripherique in Paris. *Transp. Res. B* 23, 29–47.
- Payne, H.J., 1971. Models of freeway traffic and control. In: *Bekey, G.A. (Ed.), Mathematical Models of Public Systems, Simulation Councils Proc. Ser.*, vol. 1, pp. 51–61.
- Phillips, W.F., 1978. A new continuum traffic model obtained from kinetic theory. *IEEE Transp. Autom. Control* 23, 1032–1036.
- Pipes, L.A., 1969. Vehicle acceleration in the hydrodynamic theory of traffic flow. *Transp. Res.* 3, 229–234.
- Richards, P.I., 1956. Shock waves on the highway. *Oper. Res.* 4, 42–51.
- Ross, P., 1988. Traffic dynamics. *Transp. Res. B* 22, 421–435.
- Treiber, M., Hennecke, A., Helbing, D., 1999. Derivation, properties, and simulation of a gas-kinetic-based, nonlocal traffic model. *Phys. Rev. E* 59, 239–253.
- Whitham, G.B., 1974. *Linear and Nonlinear Waves*. Wiley, New York.
- Zhang, H.M., 1998. A theory of nonequilibrium traffic flow. *Transp. Res. B* 32, 485–498.
- Zhang, H.M., 1999. Analyses of the stability and wave properties of a new continuum traffic theory. *Transp. Res. B* 33, 399–415.